PNAS
www.pnas.org

Supplementary Information for

Medin aggregation causes cerebrovascular dysfunction in aging wildtype mice

Karoline Degenhardt, Jessica Wagner, Angelos Skodras, Michael Candlish, Anna Julia Koppelmann, Katleen Wild, Rusheka Maxwell, Carola Rotermund, Felix von Zweydorf, Christian Johannes Gloeckner, Hannah A. Davies, Jillian Madine, Domenico Del Turco, Regina Feederle, Tammaryn Lashley, Thomas Deller, Philipp Kahle, Jasmin K. Hefendehl, Mathias Jucker, Jonas J. Neher

Dr. Jonas J. Neher
Email: jonas.neher@dzne.de

This PDF file includes:

www.pnas.org/cgi/doi/10.1073/pnas.2011133117

Supplementary Materials and Methods

Human tissue

Ascending aortic tissue samples (Supplementary Table S1) were rapidly frozen in dry ice and isopentane slurry after collection, and immediately stored at –80°C prior to use. For histology, the tissue was formalin-fixed and paraffin-embedded and cut into 10 µm-thick sections.

Human brain tissue (Supplementary Table S2) was obtained from the Queen Square Brain Bank for Neurological Disorders (UCL Institute of Neurology, London, UK). 12-15 µm thick, FFPE brain sections from the frontal or temporal cortex were used for analysis.

Informed consent from all patients and ethical approval was obtained for all experiments (see main text for details).

Tissue collection

For brain and aorta preparation, mice were deeply anesthetized and transcardially perfused with phosphate-buffered saline (PBS). Brain hemispheres were separated, with one hemisphere freshly frozen on dry ice for biochemical analyses and the other stored for 24 h in 4 % paraformaldehyde (PFA). The PFA-fixed hemisphere was then transferred to 30% sucrose for another 48 h, and subsequently frozen in 2-methyl-butane. Coronal sections of 25 µm or horizontal sections of 40 µm thickness were cut with a freezing sliding microtome (Leica).

After removal of the perivascular adipose tissue, the aorta was also either freshly frozen on dry ice or fixed in PFA overnight followed by paraffin embedding and microtome sectioning at 5 µm thickness. Sections were mounted on glass slides and dried at 60°C overnight.

Blood was collected from deeply anesthetized mice by cardiac puncture (before perfusion) and serum samples were obtained by coagulation at room temperature for 10 min, centrifugation for 10 min at 2,000 rpm and collection of the cell-free supernatant.

For gel electrophoresis and ELISA analyses, tissue samples were homogenized in PBS using a Precellys® lysing kit for 20 % w/v brain homogenates in Tris-HCl buffer (50 mM Tris pH 8, 150 mM NaCl, 5 mM EDTA) or 1% (w/v) aorta homogenates in PBS, containing phosphatase and protease inhibitors (Pierce). Brain homogenates were sonicated in three cycles for 35 s each, at 4°C (Bioruptor, Diagenode). Total protein concentration of homogenates was quantified using a BCA assay (Pierce).

Electron microscopy

For electron microscopy, animals were perfused with PBS, followed by a mixture of 4% PFA and 0.5% glutaraldehyde in 0.1 M cacodylate buffer (pH 7.4, Science Services) for 15 min. Serial frontal brain sections were cut with a vibratome (Leica VT1000S), washed in TBS, incubated in 0.1% $NaBH_4$ (Sigma-Aldrich), and blocked with 5% BSA for 1 h at room temperature (RT) to reduce non-specific staining. For MFG-E8 staining, goat polyclonal anti-murine MFG-E8 (R&D systems, 1:1,000) was used as primary antibody followed by a biotinylated specific anti-IgG (Vector

Laboratories, 1:200) as secondary antibody. After washing in TBS, sections were incubated in avidin–biotin– peroxidase complex (ABC-Elite; Vector Laboratories) for 90 min at RT and were reacted with diaminobenzidine (DAB) solution (Vector Laboratories) at RT. Sections were silver-intensified by incubation in 3% hexamethylenetetramine (Sigma-Aldrich), 5% silver nitrate (AppliChem), and 2.5% disodium tetraborate (Sigma-Aldrich) for 10 min at 60°C, in 1% tetrachlorogold solution (AppliChem) for 3 min, and in 2.5% sodium thiosulfate (Sigma-Aldrich) for 3 min. After staining, sections were washed in 0.1 M cacodylate buffer, osmicated (0.5% OsO4 in cacodylate buffer), dehydrated (70 % ethanol containing 1% uranyl acetate (Serva)), and embedded in Durcupan (Sigma-Aldrich). Ultrathin sections were collected on single-slot Formvar-coated copper grids that were contrast enhanced with lead citrate for 4 min and examined using a Zeiss electron microscope (Zeiss EM 900).

Anti-human Medin antibody

For the custom-made anti-human Medin antibody, rats were immunized with synthetic ovalbumin-coupled Medin peptide aa 268-287 (RLDKQGNFNAWVAGSYGNDQ). Hybridoma supernatants were screened by ELISA on biotinylated peptides and positive clones were further validated by Western blotting and IF. Clone MFGS 1H4 (rat IgG2b) was recloned by limiting dilution to obtain a stable monoclonal cell line to be used for further experiments (cell culture supernatant 1:10 WB, 1:2 IF). As isotype control, cell culture supernatant of rat IgG2b was used.

Immunohistochemistry and quantification

Paraffin sections were deparaffinized and rehydrated using standard protocols. Free-floating brain sections were washed in PBS and endogenous peroxidase was quenched by incubation of the sections with 0.3% hydrogen peroxide (AppliChem) in PBS for 30 min. For enhancement of vascular Medin and MFG-E8 staining, brain sections were pretreated with 1 µg/mL proteinase K (in 1 mM $CaCl_2$, 50 mM Tris buffer, pH 7.6) at 37°C for 30 min, followed by deactivation in 10 mM EDTA (pH 6) at 90°C for 10 min (1). Human aorta paraffin sections were boiled in citrate buffer (1.8 mM citric acid, 8.2 mM trisodium citrate, pH 6) at 90°C for 30 min. Unspecific antibody binding was blocked by incubation with 2% normal donkey serum (DS) in PBS containing 0.3% Triton X-100, and primary antibody (diluted in the same medium) was incubated at 4°C overnight with agitation, followed by washing and incubation with the secondary antibody (diluted in 1% DS-PBS) using either ABC and Peroxidase Substrate kits (Vectastain) or appropriate fluorescently labelled secondary antibodies (according to the manufacturer's instructions, Invitrogen or Jackson ImmunoResearch, 1:250). To reduce autofluorescence (from various sources such as lipofuscin, elastin or collagen) in brain sections, TrueBlack™ Quencher (Biotium) was applied (1:20 in 70% ethanol) for 5-10 s according to the manufacturer's instructions.

Primary antibodies used were an anti-human Medin antibody (clone 1H4; see above), a goat polyclonal anti-murine MFG-E8 antibody, with high affinity for the C2 domain (R&D systems,

1:1,000; cp. epitope mapping Suppl. Fig. 1), anti-SMA (Dako, 1:200), anti-AQP4 (Merck, 1:1000), anti-CD31 (BD Biosciences, 1:50). For nuclear staining, sections were incubated in Nuclear Fast Red (1%, Fluka, in 5% $AlSO_4$, Merck) for 5 min. Amyloid staining was performed using Methoxy-X04 (4% vol of 10 mg/ml in DMSO and 7.7% vol CremophorEL in 88.3% PBS) for 30 min at RT or Congo red, as described (2). For labelling of arterioles, Alexa hydrazide (1:1000 from 2 mM stock solution) was added for 90 s (3).

Images were acquired using a Zeiss Axioplan 2 with the AxioVision 4.7 software (Zeiss) using 40x/0.75 objective, with fixed camera exposure time and lamp intensity for comparative stainings. Image background was subtracted using an inbuilt Fiji plugin (Rolling-Ball background correction). Optical sections were acquired on a Zeiss LSM 510 META (Axiovert 200M) confocal microscope with a 20x/0.5 (air) or an oil immersion 40x/1.3 or 63x/1.4 objective on the LSM software 4.2 (Carl Zeiss), using sequential excitation of fluorophores (A488, A568, A647) or amyloid ligands (Methoxy-X04, Congo red). Maximum intensity projections were generated with Fiji.

For automated quantification of vascular MFG-E8, fluorescence images were acquired on a Zeiss AxioObserver.Z1 Slide Scanner, using a 20x/0.8 objective for image acquisition of whole brain sections, followed by semi-automated and blinded analysis with Fiji using custom-written plugins (available on request). For this automated, low magnification analysis, a rat monoclonal anti-murine MFG-E8 (R&D systems, 1:500) was used in combination with the anti-SMA antibody (Dako, 1:200), as this monoclonal anti-murine MFG-E8 showed higher signal in the vasculature compared to the parenchyma. Automated selection of the whole brain area as region of interest (ROI) was manually checked and corrected if necessary. Fluorescence channels for MFG-E8 and SMA were split and if needed, intensity thresholds were manually adjusted to exclude unspecific background signal. For every section, the area of MFG-E8 and SMA staining in the ROI was measured. To determine the vascular MFG-E8 signal, thresholded SMA area was converted to a binary mask and the area and intensity of the masked MFG-E8 signal was determined. For each animal, the total vascular MFG-E8 area (μm^2) was normalized to the total area of SMA (μm^2) in a random set of every 12^{th} systematically sampled coronal brain sections (excluding olfactory bulb and cerebellum).

Volume of endothelial cells and astrocytic endfeet coverage on blood vessels were determined by 3D-reconstruction (Imaris software with XTension “Surface Surface Contact Area” by Matthew Gastinger, Bitplane) of endothelial cells (CD31) and astrocytic end feet (AQP4) signal in 5 µm z-stacks (6 images in three different sections per animal, 40x/1.3 objective).

Medin purification protocol

Amyloid was extracted from human and mouse aortic tissue according to a previous published protocol for Amyloid-β purification from mouse brain (4). Briefly, 50 mg of human aortic tissue or 75 mg of pooled fresh-frozen aortas from 16 mice were homogenized in 2 ml calcium- and magnesium-free PBS using a Glass-Teflon homogenizer (total homogenate =TH). TH was then incubated with citrate lysis buffer (10 mM citrate pH 6, 1 mM EDTA, 1% wt/vol Triton X-100) for 30 min on ice. The aorta lysate (Lysed homogenate = LH) was adjusted to 18% (wt/vol) iodixanol (OptiPrep, Sigma-Aldrich) and centrifuged twice through an iodixanol gradient (SW41 Ti rotor, Beckmann, 60.000 x g, 4°C). The top layer was discarded; the next two layers and their interphases were collected (Fraction 1 and 2 = F1, F2) and diluted in citrate buffer (10 mM citrate pH 6, 137 mM NaCl, 1 mM EDTA). After centrifugation for 1 hour at 21,000 x g, the pellet was resuspended in 400 µl Tris buffer (10 mM, pH 8.3, 1.71 M NaCl) containing 1% (wt/vol) zwittergent 3-14 (P1). After centrifugation for 30 min at 135,000 x g, the supernatant was discarded, and the pellet was resuspended in 100 µl TMS buffer (50 mM Tris–HCl, pH 7.8; 100 mM NaCl, 10 mM MgCl2) and treated with 300 units/mL of Benzonase at 37°C overnight (P2). Samples were ultracentrifuged for 30 min at 135,000 x g. Residual proteins in the pellet were digested with 40 µg/ml proteinase K (Fisher Scientific) in TMS buffer for 1 h at 37 °C and stopped by the addition of 2 mM PMSF. The digested samples (P3) were adjusted to 1.71 M NaCl and centrifuged for 30 min at 135,000 x g through a 1 M sucrose layer. The pellet, P4, was then resuspended in 0.1 M sodium acetate buffer.

Cloning of MFG-E8 domains and Transfection of HEK cells

The psd44-iGFP-MFGE8-long vector (generated by A. Mariotti, Université Lausanne (5) and distributed by AddGene) was amplified for full-length MFG-E8 expression after Ex-Taq PCR and verification via gel electrophoresis (FL-MFG-E8). Additionally, the four different MFG-E8 domains (E1, E2, C1, C2) were subcloned and amplified by Ex-Taq-PCR using specifically designed primers and transformed into *E. coli* DH5α cells. Sequences were verified using BigDye Terminator v.3.1 and an ABI 3130xl Genetic Analyzer (Applied Biosystems). Primer sequences can be obtained on request. DNA of FL-MFG-E8 and its individual domains were cloned using SalI/NotI restriction sites into pCMV-3xFLAG for transfection of HEK293E cells, which were cultured in Dulbecco's modified Eagle's medium (DMEM) with 10% FCS at 37 °C in 5% CO2. Transient transfections with DNA were performed with FuGENE and OptiMEM (Roche Applied Science) following the manufacturer's instructions. HEK293E cells were lysed in RIPA buffer (50 mM Tris-HCl pH 8.0, 150 mM NaCl, 1% NP-40, 0.5% NaDesoxycholate, 0.5% SDS) and pelleted at 18,000rpm for 15 min at 4 °C. Total protein concentration of RIPA lysates was determined with the bicinchoninic acid (BCA) protein assay kit (Pierce).

Western Blotting

Samples were diluted and denatured in loading buffer (10 % glycerol, 2 % SDS, 2 % β-mercaptoethanol, 0.1 M Tris-HCl pH 8.6), boiled at 95°C for 5 min and loaded on a Tris-Tricine 10-20 % or Bis-Tris 4-12% gradient gel (Invitrogen). For detection of MFG-E8 in total homogenates, brain samples (15µg total protein per sample) were preheated for 5 min in 8M Urea at 70°C before denaturation in loading buffer. After electrophoresis, gels were transferred to a nitrocellulose membrane in a semi-dry blotting system. Transfer was confirmed by Ponceau-S staining. Blocking was performed either with 5% milk (FLAG-M2, 1H4, 6e10) or 5% donkey serum (polyclonal anti-murine MFG-E8) in PBS-T for 1 h. For detection of Medin or Aβ, membranes were boiled in PBS for 5 min at 90°C. Subsequently, membranes were incubated overnight at 4°C with the primary antibody in PBS-T. Primary antibodies used were goat polyclonal anti-murine MFG-E8 (R&D systems, 1:1,000), anti-Flag M2-Peroxidase (HRP) (Sigma, 1:30,000), anti-human Medin 1H4 (1:10) and anti-Aβ 6e10 (Covance, 1:2,500). Membranes were then probed with the respective secondary horseradish peroxidase (HRP)-labelled antibodies (1:20,000, Jackson ImmunoLaboratories). Protein bands were detected using chemiluminescent peroxidase substrate (ECL prime, GE Healthcare).

Enzyme-linked immunosorbent assay (ELISA)

Quantification of mouse MFG-E8 by ELISA (R&D Systems) in serum, aorta and brain was performed according to the manufacturer's instructions. Serum samples were pre-diluted 1:3, 20% brain homogenates 1:10 and 1% aorta homogenates 1:500 before the measurements. Protein levels were normalized to the total protein content as measured by BCA protein assay (Pierce). Measurements were performed on a FLUOstar Omega reader (BMG Labtech).

Preparation and aggregation of recombinant human Medin

Recombinant human Medin was produced as previously reported (6) and was aggregated *in vitro* at a concentration of 27 µg/ml in Tris-HCl buffer (50 mM Tris pH 8, 150 mM NaCl, 5 mM EDTA) for 48h at 37°C without agitation.

Mass spectrometry (LC-MSMS)

Prefractionation of 10% aorta homogenates in PBS was performed via SDS-polyacrylamid gel electrophoresis according to standard methods on the Invitrogen NuPAGE system (10% gel). The separated proteins were fixed in 50% MeOH containing 12% acetic acid for 30 min followed by staining with 0.4% Coomassie Brilliant Blue G250 prior to dissection of gel bands of <17 kDa protein size. Protein bands were de-stained and washed by incubation in 40% acetonitrile in HPLC grade water for 20 min and shortly dehydrated in 100% acetonitrile. Dried gel plugs were exposed to 5 mM DTT for 15 min at 60°C, which was replaced by 25 mM iodacetamid for 45 min at ambient temperature in the dark. Washing with 40% and 100% acetonitrile was repeated. After drying,

proteins were subjected to in-gel proteolysis using trypsin (Sigma-Aldrich, 10 ng/µl in 50 mM ammonium bicarbonate buffer) over night at 37°C. Peptides were extracted by subsequent incubation of the gel plugs in 2.5% trifluoracetic acid (TFA), 0.5% TFA in 50% acetonitrile and 0.5% TFA in 100% acetonitrile each for 15 min at room temperature and concentrated via Speed Vac (35°C, vacuum).

Extracted peptides were analyzed by LC/MSMS using a nanoflow HPLC system (Ultimate 3000 RSLC; Thermo Fisher) coupled to an Orbitrap Q-Excative (Thermo Fisher) tandem mass spectrometer. Peptides were separated by reversed C-18 chromatography and 180-min gradients. MS1 spectra were acquired in the Orbitrap at 70K resolution. After selection of the 10 most intense precursor ions from the MS1 scans for HCD fragmentation (Top 10 method), MS2 spectra were acquired at 17.5K. For database search, tandem mass spectra were extracted by MSConvert (ProteoWizard version 3.0.7331). Charge state deconvolution and de-isotoping were not performed. All MS/MS samples were analyzed using Mascot (Matrix Science; version 2.5.1). Mascot was set up to search the SwissProt database (version 2019_08, selected for either homo sapiens [20431 entries] or mouse [17030 entries]) assuming the proteolytic enzyme trypsin. Mascot was searched with a fragment ion mass tolerance of 0.60 Da and a parent ion tolerance of 10.0 PPM. Carbamidomethyl of cysteine was specified in Mascot as a fixed modification. Deamidation of asparagine and glutamine, oxidation of methionine were specified in Mascot as variable modifications. Scaffold (version 4.4.5, Proteome Software Inc.) was used for downstream analysis and visualization.

2-photon imaging of vascular function

Cranial window surgeries were carried out as previously described in detail (7–9). Briefly, animals were anaesthetised (fentanyl, 0.05 mg / kg; midazolam, 5 mg / kg; medetomidine, 0.5 mg / kg) and a circular cranial window (4 mm diameter) was placed over the right somatosensory cortex hindlimb region. A titanium ring was then positioned over the cranial window, allowing for precise fixation of the cranial window at the 2-photon imaging setup. After completion of surgery, anaesthesia was terminated via an i.p. injection of antidote (atipamezole, 2.5 mg / kg; flumazenil, 0.5 mg / kg).

For *in vivo* 2-photon imaging, mice were anaesthetised (isoflurane; 5 % for induction, 1 - 1.5 % for maintenance) and administered an i.v. injection of fluorescein-conjugated dextran in sterile saline (70 kDa; Sigma Aldrich 46945) to visualise the cerebrovasculature as described previously (9). The mouse was then secured in a custom head-fixation device (8) positioned underneath the objective lens at the imaging setup. Imaging was performed using a motorized custom 2-photon microscope (10) equipped with a Chameleon Ultra II laser (Coherent). Motor control and image acquisition were controlled using an MP285A (Sutter Instrument Company) and ScanImage software (Vidrio Technologies). 2-photon excitation of fluorescein-conjugated dextran was performed at 800 nm (laser power <50 mW). Emission was detected using a non-descanned detector (Hamamatsu Photonics), a T560lpxr-UF2 dichroic and an ET525/50m-2p bandpass filter

(Chroma Technology Corporation). Z-stack images (512 x 512, 2 µm steps) were taken using either a Plan-Apochromat 5x/0.16 (Zeiss) or a HC Fluotar 25x/0.95 W (Leica Microsystems) objective. Line scans (positioned perpendicularly across the arterioles within the somatosensory cortex hindlimb region) were acquired using the 25x objective at 99.99 Hz using the arbitrary line scan function in ScanImage. A 50 s recording was taken for each vessel analyzed. Mechanical stimulation of the left hindlimb was triggered 5 s after the start of each recording as a single pulse using a Master-9 pulse stimulator (A.M.P.I), with a minimum interval of 2 min between subsequent hindlimb stimulations.

For quantification, the 16-bit fluorescence intensity signal along the line over the scan time was visualized in ImageJ in the form of a 2-dimensional image ('kymograph') (11). A custom-made plugin was written in ImageJ to automatically import the data to kymographs, apply a Gaussian Blur filter of 3 pixel radius to remove spike noise and threshold the resulting image using an automated threshold based on Shannon's entropy. Pixels of the resulting binary image of the kymograph were added along the time-dimension, creating a sequence of values that constitute the vessel diameter changes over the scan time. In order to render the data comparable across ROIs and animals, they were normalized to a scale of 0 to 1. To exclude higher frequency artifacts, as well as breathing and heartbeat capillary changes, the normalized data were further filtered using MATLAB. Using the Fourier power spectrum, we could determine a prominent frequency of 0.8 Hz and a subsequently broad high-frequency component thereafter. We thus designed a low-pass filter to attenuate frequencies higher than 0.75 Hz. The filtered data were time-shifted to correct for the low-pass filter phase response (group delay). The area under the curve of the filtered capillary diameter changes over time were further calculated in MATLAB, by approximating the curve integral via the trapezoidal method. Finally, in order to calculate the initial response of the blood vessels, the time constant $t_{1/2}$ of the response was obtained using a One-phase exponential fit directly implemented in GraphPad Prism, on the first 5 s of the normalized filtered capillary diameter change curves.

As it is currently not possible to label Medin deposits during *in vivo* imaging, arterioles of similar diameter were selected at random from the MCA territory. For this reason, we considered each blood vessel as an independent measurement, as we observed strong intra-individual differences in wildtype animals that may result from the presence/absence of Medin deposits, which we found to be unevenly distributed throughout the blood vessels.

TANGO analysis

The TANGO algorithm (12) was used to predict β-aggregation propensity of the Medin peptide. For this calculation the following parameters were chosen: pH 7.4, temperature 298.15 K, ionic strength 0.02 M and 1 mM concentration.

Statistics

Statistical analysis was performed using Prism 6 software. Data were tested for normal distribution (Shapiro-Wilk test) and statistical outliers were identified and removed (ROUT method). If data were normally distributed, ANOVA was performed, followed by Tukey's multiple comparison test. If data were not normally distributed, a non-parametric test (Kruskal-Wallis) was performed, followed by multiple comparison of the mean ranks with Dunn's correction if $P<0.05$. As we did not observe differences between male and female animals regarding Medin/MFG-E8 levels/deposition etc., we did not test further for gender effects in any of our analyses. All data shown are means ± S.E.M.

Linear regressions to analyze the impact of aging on vascular accumulation of MFG-E8/Medin were generated using JMP software (version 14.2.0). If necessary, data were first log10 transformed to achieve a normal distribution. Data were then analyzed using the 'Fit model' function, generating residual vs. leverage plots, where a least squares line (red) and confidence bands (shaded red) provide a visual representation of the statistical significance (at the 5% level) of the effect of X ("Age"); a significant effect is evident by the crossing of the confidence lines (shaded red/red) through the blue line in the graph in the graph, which indicates the mean of the Y leverage residuals. To calculate the data points in the graph, the mean value of Y is added to the Y-residuals and the mean of the X-value is added to the X-residuals, generating "leverage residuals", and these pairs of residuals are then used to generate the effect leverage plots shown (see e.g. [13]).

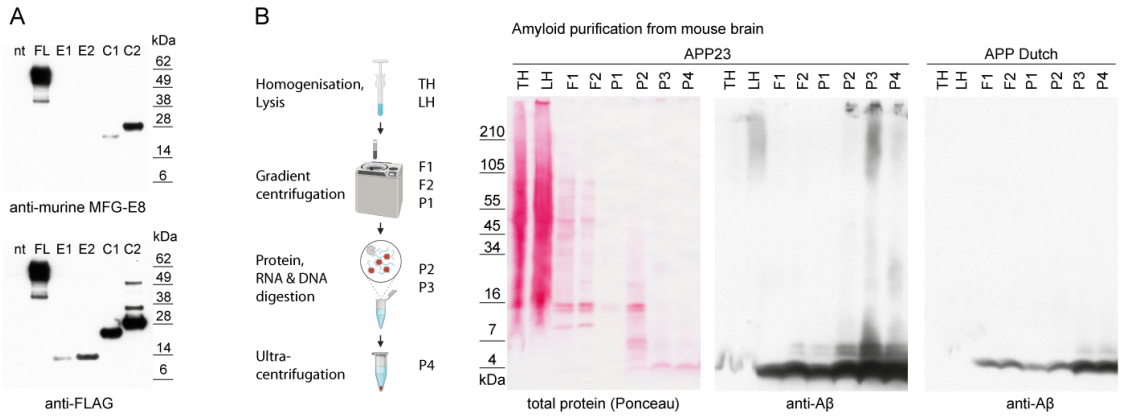

Fig. S1: Epitope mapping of the polyclonal anti-murine MFG-E8 antibody used throughout this study and amyloid extraction from transgenic mouse brain.

A, *top*: Western blotting of recombinantly expressed full-length (FL) MFG-E8 and its individual domains (E1, E2, C1, C2) demonstrates that the polyclonal anti murine-MFG-E8 antibody has the highest affinity for epitope(s) within the Medin-containing C2 domain, with low affinity also for the C1 domain and no detection of the E1 and E2 domains. *bottom,* Input control using the FLAG-tag of recombinantly expressed proteins. **B**, *left:* Graphical summary of the purification procedure for the enrichment of amyloids from tissue homogenates. *Right*, Proof-of-principle experiment demonstrating the elimination/digestion of soluble proteins during the procedure (Ponceau staining of total protein) while enriching amyloid-β from APP23 and APP Dutch transgenic mouse brains (anti-Aβ staining).

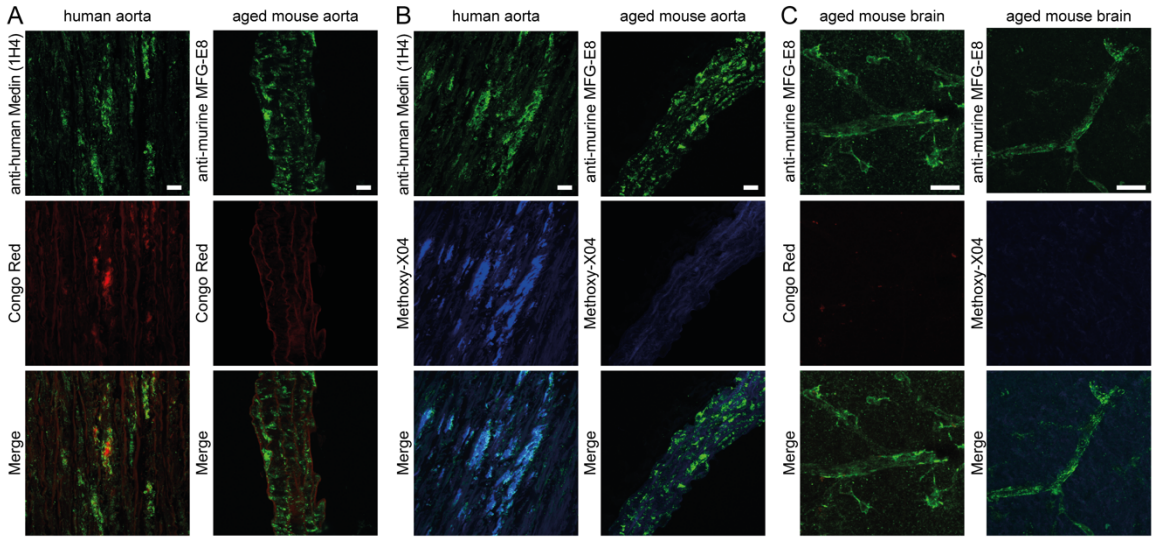

Fig. S2: Lack of affinity for amyloid dyes in the aged mouse aorta and brain.

A/B, The amyloid binding dyes Congo Red (A) and Methoxy-X04 (B) stain Medin+ aggregates in the human aorta but not MFG-E8+ aggregates the aged mouse aorta. **C**, In the aged mouse brain, MFG-E8+ vascular aggregates are not stained by Congo Red or Methoxy-X04 (cp. Fig. 3 for human brain). Scale bar: 20 µm.

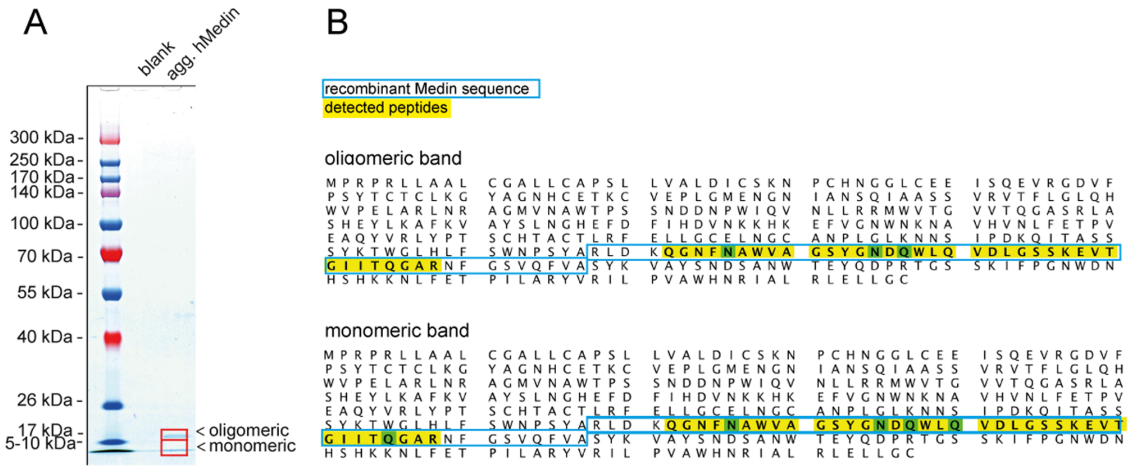

Fig. S3*:* **Mass spectrometry analysis of aggregated recombinant human Medin.**
Recombinant human Medin (hMedin) was aggregated for 48 h at 37°C and **A**, pre-fractionated by gel electrophoresis, showing monomeric and oligomeric bands, which were excised and analyzed by **B**, mass spectrometry. The coverage of the recombinant Medin sequence (blue frame) by detected peptides is marked in yellow (green= post-translational modification i.e. deamidation).

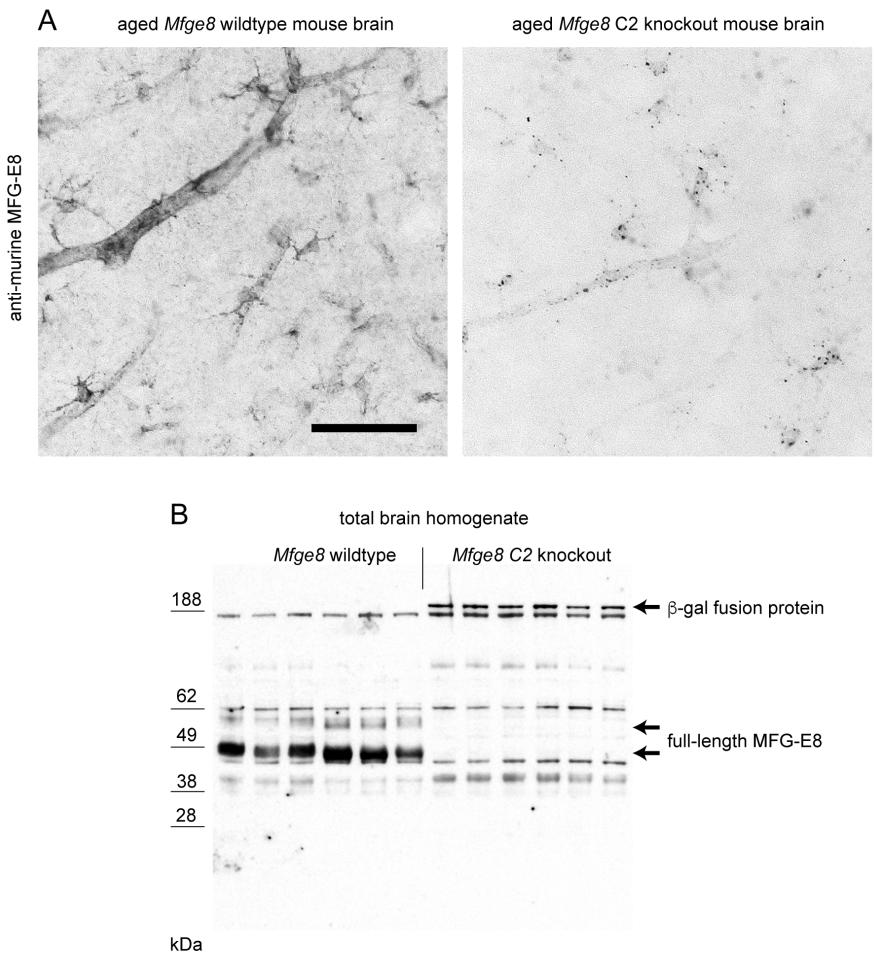

Fig. S4: MFG-E8 is retained within cells in Mfge8 C2 knockout animals

A, MFG-E8 staining in aged wildtype brain (>20-month-old) is widespread and evident both in blood vessels as well as astrocytes. In contrast, *Mfge8* C2 KO animals show only a punctate intracellular staining pattern (in parenchymal as well as vascular cells; a blood vessel is recognizable in the center of the image), in line with retention of the MFG-E8/β-galactosidase fusion protein inside the cells, resulting from the introduction of a transmembrane domain (cp. Fig. 1). **B**, Western Blotting of total brain homogenate. In wildtype animals two isoforms of the full-length MFG-E8 protein are clearly visible as two distinct bands ~50/60 kDa, but are absent in *Mfge8* C2 KO animals, where the fusion protein appears as a distinct band ~200 kDa. Scale bar = 50 µm.

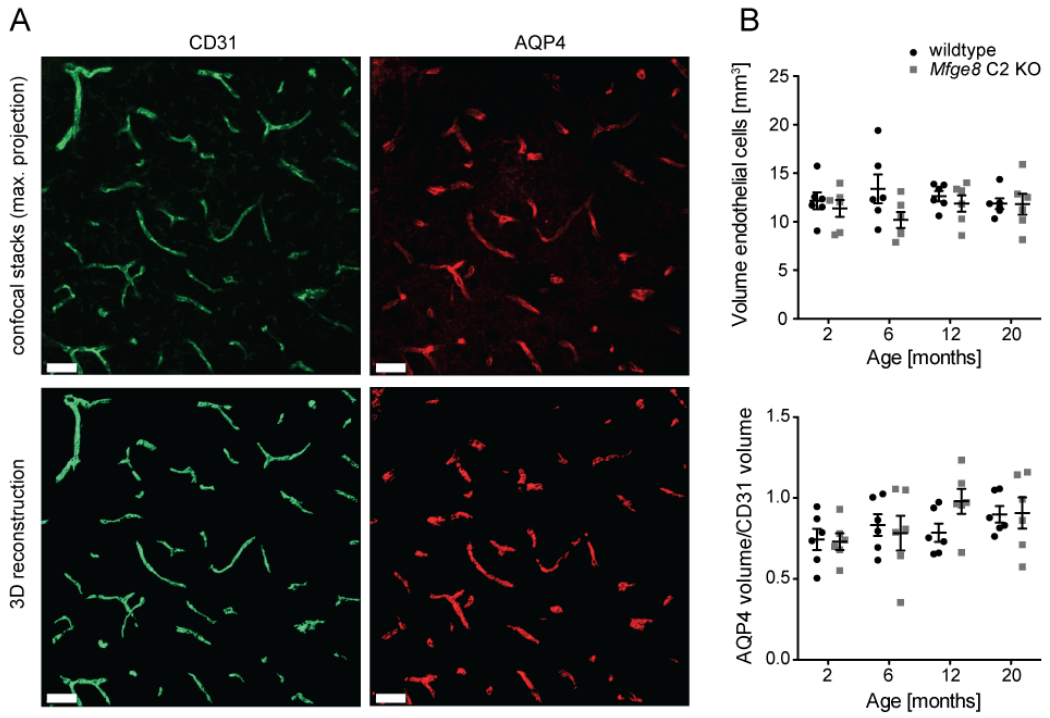

Fig. S5: Astrocytic endfeet coverage of brain blood vessels does not change with age or *Mfge8* C2 knockout.

A, Anatomically matched brain sections of wildtype and *Mfge8* C2 KO animals (3 sections per mouse with 3 males and 3 females per age group) were stained for endothelial cells (CD31) and astrocytic endfeet (Aquaporin-4, AQP4). Confocal z-stacks (5 µm; 6 per animal; *top images*) were acquired and 3D-reconstructed using Imaris software (*bottom images*) to quantify **B**, the volume of endothelial cells (*top*) and the astrocytic endfeet coverage (AQP4) of endothelial cells (*bottom*). Scale bar: 30 µm.

Table S1: Patient information of aorta donors

Case	Age (years)	Sex	Clinical presentation	Tissue source	Histology	Extraction
Patient 1	69	F	Aneurysm	Surgery	X	X
Patient 2	70	F	Cardiac arrest, hypoxic brain injury	Post-mortem	X	
Patient 3	67	M	Aneurysm	Surgery	X	X
Patient 4	81	F	Aneurysm	Surgery		X

Table S2: Patient information of brain donors

Case	Age (years)	Sex	Clinical presentation	Braak and Braak	CERAD	THAL	ABC score
Patient 5	80	F	Normal/ path ageing	2	none	0	A0B1C0
Patient 6	86	F	Normal/ path ageing	2	none	0	A0B1C0
Patient 7	84	M	Control	0	none	0	A0B0C0

SI References

1. H. Kai, *et al.*, Enhanced Antigen Retrieval of Amyloid β Immunohistochemistry: Re-evaluation of Amyloid β Pathology in Alzheimer Disease and Its Mouse Model. *J. Histochem. Cytochem.* **60**, 761–769 (2012).
2. S. Peng, *et al.*, Role of aggregated medin in the pathogenesis of thoracic aortic aneurysm and dissection. *Lab. Invest.* **87**, 1195–1205 (2007).
3. Z. Shen, Z. Lu, P. Y. Chhatbar, P. O'Herron, P. Kara, An artery-specific fluorescent dye for studying neurovascular coupling. *Nat. Methods* **9**, 273–276 (2012).
4. J. Stohr, *et al.*, Purified and synthetic Alzheimer's amyloid beta (Abeta) prions. *Proc. Natl. Acad. Sci. U. S. A.* **109**, 11025–11030 (2012).
5. C. Carrascosa, *et al.*, MFG-E8/lactadherin regulates cyclins D1/D3 expression and enhances the tumorigenic potential of mammary epithelial cells. *Oncogene* **31**, 1521–1532 (2012).
6. H. A. Davies, *et al.*, Oxidative Stress Alters the Morphology and Toxicity of Aortic Medial Amyloid. *Biophys. J.* **109**, 2363–2370 (2015).
7. J. K. Hefendehl, *et al.*, Long-term in vivo imaging of β-amyloid plaque appearance and growth in a mouse model of cerebral β-amyloidosis. *J. Neurosci.* **31**, 624–629 (2011).
8. J. K. Hefendehl, *et al.*, Repeatable target localization for long-term in vivo imaging of mice with 2-photon microscopy. *J. Neurosci. Methods* **205**, 357–363 (2012).
9. P. Füger, *et al.*, Microglia turnover with aging and in an Alzheimer's model via long-term in vivo single-cell imaging. *Nat. Neurosci.* **20**, 1371–1376 (2017).
10. D. G. Rosenegger, C. H. T. Tran, J. LeDue, N. Zhou, G. R. Gordon, A High Performance, Cost-Effective, Open-Source Microscope for Scanning Two-Photon Microscopy that Is Modular and Readily Adaptable. *PLoS One* **9**, e110475 (2014).
11. K. Kisler, *et al.*, In vivo imaging and analysis of cerebrovascular hemodynamic responses and tissue oxygenation in the mouse brain. *Nat. Protoc.* **13**, 1377–1402 (2018).
12. A.-M. Fernandez-Escamilla, F. Rousseau, J. Schymkowitz, L. Serrano, Prediction of sequence-dependent and mutational effects on the aggregation of peptides and proteins. *Nat. Biotechnol.* **22**, 1302–1306 (2004).
13. J. Sall, Leverage Plots for General Linear Hypotheses. *Am. Stat.* **44**, 308–315 (1990).